Stability of excited states of a Bose-Einstein condensate in an anharmonic trap

Dmitry A. Zezyulin* and Georgy L. Alfimov†
Moscow Institute of Electronic Engineering, Zelenograd, Moscow, 124498, Russia

Vladimir V. Konotop‡
Centro de Física Teórica e Computacional, Universidade de Lisboa, Complexo Interdisciplinar, Avenida Professor Gama Pinto 2, Lisboa 1649-003, Portugal
and Departamento de Física, Faculdade de Ciências, Universidade de Lisboa, Campo Grande, Edifício C8, Piso 6, Lisboa 1749-016, Portugal

Víctor M. Pérez-García§
Departamento de Matemáticas, E. T. S. I. Industriales, and Instituto de Matemática Aplicada a la Ciencia y la Ingeniería, Universidad de Castilla-La Mancha, 13071 Ciudad Real, Spain
(Received 6 March 2008; published 3 July 2008)

We analyze the stability of nonground nonlinear states of a Bose-Einstein condensate in the mean-field limit in effectively one-dimensional ("cigar-shape") traps for various types of confining potentials. We find that nonlinear states become, in general, more stable when switching from a harmonic potential to an anharmonic one. We discuss the relation between this fact and the specifics of the harmonic potential which has an equidistant spectrum.

DOI: 10.1103/PhysRevA.78.013606 PACS number(s): 03.75.Lm, 05.45.Yv, 42.65.Tg

I. INTRODUCTION

The mean-field theory of a Bose-Einstein condensate (BEC) is based on the Gross-Pitaevskii equation (GPE) [1–3]

$$i\Psi_t = -\Delta\Psi + V(\mathbf{x})\Psi - \sigma|\Psi|^2\Psi, \tag{1}$$

for the macroscopic wave function $\Psi=\Psi(t,\mathbf{x})$. This model describes accurately the behavior of an ultracold condensed atomic cloud trapped by an external potential $V(\mathbf{x})$. In the dimensionless variables of Eq. (1) the Planck constant is equal to one, $\hbar=1$, and the atomic mass is $m=1/2$. The parameter σ stands for the sign opposite that of the scattering length a_s: $\sigma=-\text{sign}(a_s)$. An important class of solutions of GPEs are stationary nonlinear modes defined as

$$\Psi(t,\mathbf{x}) = e^{-i\omega t}\psi(\mathbf{x}), \tag{2}$$

with the boundary conditions

$$\psi(\mathbf{x}) \to 0 \quad \text{as} \quad |\mathbf{x}| \to \infty. \tag{3}$$

In this case $\psi(\mathbf{x})$ satisfies the equation

$$\Delta\psi + [\omega - V(\mathbf{x})]\psi + \sigma\psi^3 = 0. \tag{4}$$

The nonlinear eigenvalue ω is called the chemical potential in the context of BEC applications. The *ground state* solutions of Eqs. (3) and (4) [i.e., positive solutions which minimize the energy functional for Eq. (1)] are of primary importance for BEC applications [4]. Apart from them some *nonground* nonlinear modes have also been studied (see, e.g., [5–10]). However, all of the practical applications of high order modes are linked to their experimental feasibility, which requires stability. The stability of high order modes has already been studied in the case of a harmonic potential $V(\mathbf{x})=|\mathbf{x}|^2$. The one-dimensional case was studied in Refs. [10–13] while multidimensional solutions were considered in Refs. [14–22].

However, to the best of our knowledge, the relation between the stability properties of nonlinear modes and the specific forms of the confining potential $V(\mathbf{x})$ has not been discussed, previously. This is a problem of significant practical importance since high order modes can be used for generation of nonlinear coherent structures, such as, for example, solitonic trains in a quasi-one-dimensional limit (see e.g., [10]).

In this paper we study how the shape of the potential $V(x)$ governs the stability properties of nonlinear modes. In our study and to simplify the analysis we will consider a quasi-one dimensional geometry modeled by a one-dimensional GPE [23]

$$i\Psi_t = -\Psi_{xx} + V(x)\Psi - \sigma\Psi|\Psi|^2. \tag{5}$$

In that situation, Eq. (4) becomes

$$\psi_{xx} + [\omega - V(x)]\psi + \sigma\psi^3 = 0. \tag{6}$$

We will show that the harmonic potential $V(x)=x^2$ corresponds to a very peculiar situation related to the fact that in the linear limit this potential has an equidistant spectrum. We will discuss how switching from the harmonic potential to an anharmonic one makes higher nonlinear modes "more stable" and even a "weak" anharmonicity [say, $V(x)=x^2+\kappa x^4$, $|\kappa|\ll 1$] is enough to change drastically the stability properties of high-order nonlinear modes.

It is relevant to point out that the nonlinearity introduces not only mathematical difficulties for the study of the eigenmode problem, but significantly diversifies the list of physi-

*d.zezyulin@gmail.com
†galfimov@yahoo.com
‡konotop@cii.fc.ul.pt
§victor.perezgarcia@uclm.es

cally relevant limiting cases. Indeed, the linear case has *two* characteristic scales: the de Broglie wavelength and the scale of the potential. In our notations, the first one is $\lambda \sim \max_x|\psi_x|/\max_x|\psi|$; the scale of the potential, roughly speaking coincides with the classically allowed domain (in what follows denoted as x_d). The nonlinearity introduces a *third* relevant scale $\ell \sim 1/\max_x|\psi|$. For repulsive nonlinearities this scale corresponds to the healing length [1], while in the case of attractive nonlinearities it measures the width of a matter-wave soliton. Therefore the diversity of limiting cases of the nonlinear eigenvalue problem is characterized by the interplay between the parameters λ, x_d, and ℓ.

The paper is organized as follows. In Sec. II we describe the typical structure of the families of nonlinear modes and formulate the stability problem. The results for the harmonic potential are summarized in Sec. III. Next, we turn to the consideration of the anharmonic potentials $V(x)=x^2+\kappa x^4$ (Sec. IV) and $V(x)=x^4$ (Sec. V). The last section (Sec. VI) contains some additional discussions and a summary of our results.

II. DEFINITIONS AND PREVIOUS RESULTS

A. Branches of nonlinear modes

In the small amplitude limit $\psi \to 0$, the cubic term in Eq. (6) can be neglected and the solutions can be approximated by the eigenfunctions $\tilde{\psi}_n(x)$, $n=0,1,\ldots$ of the linear eigenvalue problem

$$\psi_{xx} + [\omega - V(x)]\psi = 0. \tag{7}$$

It is assumed that the potential $V(x)$ is nonsingular, bounded from below, and $V(x) \to \infty$ as $|x| \to \infty$, so that the spectrum of Eq. (7) is discrete. Throughout this paper we will deal with even potentials, $V(x)=V(-x)$. The real eigenfunctions of Eq. (7), we denote them $\tilde{\psi}_n(x)$ with $n=0,1,\ldots$, constitute an orthonormal set:

$$\langle \tilde{\psi}_n, \tilde{\psi}_m \rangle \equiv \int_{-\infty}^{\infty} \tilde{\psi}_n(x)\tilde{\psi}_m(x)dx = \delta_{m,n} \tag{8}$$

(here $\delta_{m,n}$ is the Kronecker delta).

It will be convenient to describe the families of nonlinear modes in terms of bifurcation diagrams in the plane (ω, N) where

$$N = \int_{-\infty}^{\infty} \psi^2(x)dx \tag{9}$$

corresponds to the number of particles. Then, the respective eigenvalues of Eq. (7), $\omega=\tilde{\omega}_n$, $n=0,1,\ldots$, are the points of bifurcation where families of nonlinear modes of Eq. (6), to be denoted as $\Gamma_0,\Gamma_1,\Gamma_2,\ldots$, branch off from the zero solution $\psi(x)\equiv 0$ [6,31]. The branching off takes place for both cases, $\sigma=1$ (attractive nonlinearity) and $\sigma=-1$ (repulsive nonlinearity). Therefore we will label the branches of nonlinear modes in the corresponding cases by $\Gamma_n^{(a)}$ and $\Gamma_n^{(r)}$. At the same time, in the statements which are applicable to both cases $\sigma=\pm 1$, we omit the superscript writing simply Γ_n. Two examples of diagrams for $V(x)=x^2$ and $V(x)=x^4$ are shown in Fig. 1. Following [8] we call the modes described above *modes with linear counterpart*, since they can be viewed as modes of a linear oscillator "deformed" by the action of the nonlinearity.

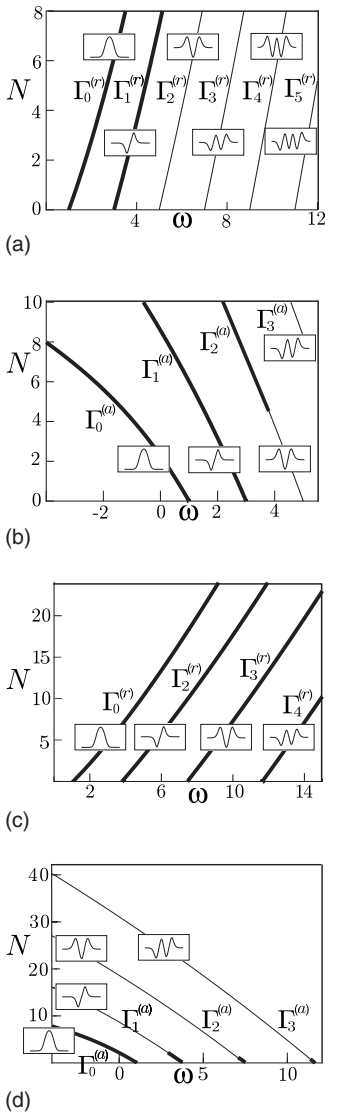

FIG. 1. (a) and (b) The lowest branches of the nonlinear modes of Eq. (6) for the potential $V(x)=x^2$ for repulsive ($\sigma=-1$) (a) and attractive ($\sigma=1$) (b) nonlinearities, respectively. (c) and (d) The same branches but for $V(x)=x^4$. All the modes bifurcate from the linear harmonic oscillator modes corresponding to the limit $N \to 0$. The fragments of curves corresponding to stable solutions are shown in bold.

A simple analysis shows that in the vicinity of a bifurcation point, say $\omega=\tilde{\omega}_n$, the small-amplitude solution of Eq. (6) for the branch Γ_n can be described by the asymptotic expansions

$$\psi_n(x) = \varepsilon\tilde{\psi}_n(x) + o(\varepsilon), \tag{10a}$$

$$\omega_n = \tilde{\omega}_n - \varepsilon^2\sigma\Omega_n + o(\varepsilon^2), \tag{10b}$$

where $\varepsilon \ll 1$ is a small parameter and the coefficient Ω_n is given by

$$\Omega_n = \int_{-\infty}^{\infty} \tilde{\psi}_n^4(x)dx. \tag{11}$$

From the physical point of view, Ω_n describes the two-body interactions, and thus defines the characteristic scale ℓ. Hence the limit described by Eq. (10) in physical terms can be defined as $\ell \ll \lambda$. We observe that this limit can be achieved not only due to small numbers of condensed particles, expressed by the condition $\varepsilon \ll 1$ [due to the normalization (8)], but also for large enough n, since $\Omega_n \to 0$ as n grows. For instance, for the case $V(x)=x^2$ we have [24]

$$\Omega_n = O(n^{-1/12}). \tag{12}$$

B. Physical units

Throughout this paper the nonlinear modes will be characterized mainly in terms of the number of particles N and the mode frequencies ω. Since we will be interested in applications of our results to the BEC mean-field theory while our analysis will be carried out in dimensionless units, before going into details we outline the link of our variables with experimentally feasible parameters. To this end we notice that the dimensionless form of Eq. (6) corresponds to the situation where the distance and time are measured, respectively, in units of a_0 and $2/\omega_0$, where a_0 is the longitudinal length of the trap and $\omega_0=\hbar/(ma_0^2)$, with m being the atomic mass, is the "effective" longitudinal trap frequency (in the case of a parabolic potential it is the real frequency of the trap, while a_0 is the linear oscillator length). In the chosen scaling the energy is measured in the units $\hbar\omega_0/2$. Then it is straightforward algebra to ensure that the link between the real, i.e., physical, number of particles $\mathcal{N}$ and the norm of the solution N (also referred to as number of particles) introduced by Eq. (9) is given by the formula $\mathcal{N}=(a_\perp/4\sqrt{2}\pi|a_s|)N$, where $a_\perp$ is the transverse linear oscillator lengths and a_s is the s-wave scattering length. In this last formula, as well as in the reduction of the three-dimensional (3D) Gross-Pitaevskii equation to the one-dimensional (1D) model (6), we have assumed that the trap is cigar-shaped, i.e., $a_\perp \ll a_0$, and that in the transverse direction the trap is harmonic. Now it is not difficult to estimate that, for example, for a trap with characteristic values $a_0 \sim 1$ mm, $a_\perp \sim 10$ μm, and $a_s \sim 5$ nm, a unit of the norm N corresponds to $\mathcal{N} \sim 10^2$ atoms, or to the mean atomic density $\sim 0.4 \times 10^9$ cm^{-3}.

C. Quasiclassical quantization

The limit of large N and small local densities $|\psi|^2 \ll 1$, denoted nonlinear WKB approximation [9], allows for an analytical construction of explicit solutions. Let us consider $V(x)=x^{2d}$, where d is a positive integer and assume that $N \gg 1$, or more precisely, that $\delta=N^{-1-1/d} \ll 1$. Bound states corresponding to sufficiently large ω, specifically $E=\omega N^{-2} \gtrsim 1$, correspond to an atomic cloud distributed over a large spatial domain roughly determined by the classical turning points, $\pm x_d = \pm \omega^{1/2d}$. Since x_d grows with ω, one can reach the levels corresponding to sufficiently low densities of particles, i.e., the quasilinear limit.

Returning to the definition of modes with a linear counterpart, the arguments presented in this section allow one to conjecture that *only modes with a linear counterpart can exist in the limit* $\omega \to \infty$ at N fixed. To describe that situation, we focus on the repulsive case $\sigma<0$, introduce an independent variable $\zeta=\delta^{1/(1+d)}x$ and a renormalized macroscopic wave function $\phi(\zeta)=\delta^{(d-1)/2(d+1)}\psi(x)$, and rewrite Eq. (6) as follows:

$$\delta^2\phi_{\zeta\zeta} + (E-\zeta^{2d})\phi - \delta\phi^3 = 0. \tag{13}$$

Since now $\delta \ll 1$ Eq. (13) is a convenient representation of the stationary eigenvalue problem for the application of the nonlinear WKB approximation. Skipping details, which can be found in [9], here we present the equation implicitly defining the diagram in the plane (E,δ):

$$E^{(1+d)/2d} \approx \frac{\delta}{A_d}\left\{\pi\left(n+\frac{1}{2}\right) + \frac{2B_d}{\sqrt{E}}\ln\left(\frac{32E}{\delta}\right) - C_d E^{(-1+d)/2d} + \arg\left[\Gamma^2\left(1-i\frac{B_d}{\sqrt{E}}\right)\right]\right\}. \tag{14}$$

Here n stands for the energy level and we introduced the constants

$$A_d = \left[\int_{-1}^{1}\sqrt{1-y^{2d}}dy\right]^{-1},$$

$$B_d = \frac{1}{2d}\left[\int_{-1}^{1}\frac{dy}{\sqrt{1-y^{2d}}}\right]^{-1}, \quad \text{for } d=1,2,\ldots,$$

$$C_d = 3B_d\sum_{k=1}^{d-1}\left\{\frac{1}{2}\cos\left(\frac{k\pi}{d}\right)\ln\left[\frac{1-\cos\left(\frac{k\pi}{d}\right)}{1+\cos\left(\frac{k\pi}{d}\right)}\right] - \sin\left(\frac{k\pi}{d}\right)\arctan\left[\sin\left(\frac{k\pi}{d}\right)\right]\right\} \quad \text{for } d=2,3,\ldots$$

and $C_1=0$. $\Gamma(\cdot)$ is the standard notation for the gamma function [25].

Solutions of the transcendental Eq. (14) with respect to the energy E at fixed δ and n give the eigenvalues (energy levels). According to the previous discussion, when $E \to \infty$ one recovers the WKB formula for the energy levels of the potential $V(x)=x^{2d}$. While for the case of the harmonic oscillator the form of Eq. (14) can be found in Ref. [9], for the situation of our particular interest below, $d=2$, the limit $E \to \infty$ (and thus $n \to \infty$) of the nonlinear WKB equation (14) acquires the form

$$E_n^{3/4} = \frac{2\sqrt{2}}{3}K\left(\frac{1}{\sqrt{2}}\right)\delta\left[\pi\left(n+\frac{1}{2}\right) + \frac{\ln n}{2\sqrt{2\pi}K\left(\frac{1}{\sqrt{2}}\right)\sqrt{n}} + O\left(\frac{1}{\sqrt{n}}\right)\right], \tag{15}$$

where $K(\cdot)$ is the complete elliptic integral of the first kind [25].

Considering the last two terms in the expansion of the energy levels (15) as a perturbation for n large enough, and

neglecting them in the leading order, in the remaining part of the expression for E_n one readily recognizes the familiar Bohr-Sommerfeld quantization condition. Thus formula (15) can be viewed as the nonlinear generalization of the standard quasiclassical quantization well-known in the quantum mechanics.

D. Stability problem (general)

Consider now the stability problem for the modes corresponding to a fixed branch Γ_n. Let $\psi_n(x)$ be a solution of Eq. (6) corresponding to ω_n. Following the standard procedure we represent $\Psi(x,t)=[\psi_n(x)+\xi(x,t)]e^{-i\omega_n t}$, linearize the dynamical equation with respect to $\xi(x,t)$, and arrive at the equation

$$i\xi_t = -\xi_{xx} - [\omega_n - V(x)]\xi - \sigma\psi_n^2(2\xi + \xi^*),$$

where the asterisk stands for the complex conjugation. Decomposing $\xi(x,t)$ into real and imaginary parts, $\xi(x,t)=\chi(x,t)+i\varphi(x,t)$ we obtain

$$\chi_t = -L_n^- \varphi,$$

$$\varphi_t = L_n^+ \chi, \tag{16}$$

where

$$L_n^+ = L_n + 3\sigma\psi_n^2(x),$$

$$L_n^- = L_n + \sigma\psi_n^2(x),$$

and

$$L_n = \frac{d^2}{dx^2} + \omega_n - V(x).$$

It follows from Eq. (16) that stability of the nonlinear mode is determined by the spectrum of the following eigenvalue problem:

$$L_n^- L_n^+ \zeta = \Lambda\zeta. \tag{17}$$

Since the operator L_n^- is degenerate [the kernel of this operator contains at least the function $\psi_n(x)$], the eigenvalue problem (17) has a zero eigenvalue. Then if the remainder of the spectrum of $L_n^- L_n^+$ is *real* and *non-negative* then the nonlinear mode $\Psi(x,t)=e^{-i\omega_n t}\psi_n(x)$ is said to pass the linear stability test. The presence of *negative* or *complex* eigenvalues in the spectrum of $L_n^- L_n^+$ implies the linear instability of this mode.

E. Stability problem (small amplitude modes)

If ω_n lies close to a bifurcation point $\tilde{\omega}_n$ then the spectrum of the operator $L_n^- L_n^+$ can be analyzed by means of the asymptotic expansions (10). Specifically,

$$L_n^+ = \mathcal{L}_n + \sigma\varepsilon^2[3\tilde{\psi}_n^2(x) - \Omega_n] + o(\varepsilon^2), \tag{18}$$

$$L_n^- = \mathcal{L}_n + \sigma\varepsilon^2[\tilde{\psi}_n^2(x) - \Omega_n] + o(\varepsilon^2), \tag{19}$$

$$L_n^- L_n^+ = \mathcal{L}_n^2 + \varepsilon^2\sigma M_n + o(\varepsilon^2), \tag{20}$$

where

$$\mathcal{L}_n = \frac{d^2}{dx^2} + \tilde{\omega}_n - V(x), \tag{21}$$

$$M_n = 3\mathcal{L}_n\tilde{\psi}_n^2(x) + [\tilde{\psi}_n^2(x) - 2\Omega_n]\mathcal{L}_n. \tag{22}$$

The operator $\mathcal{L}_n$ is self-adjoint and its spectrum consists of eigenvalues $\lambda_{n,k}=\tilde{\omega}_n-\tilde{\omega}_k$, $k=0,1,2,\ldots$. In the limit $\varepsilon=0$ one has the operator $L_n^- L_n^+=\mathcal{L}_n^2$ and its spectrum becomes $\Lambda_{n,k}=(\tilde{\omega}_n-\tilde{\omega}_k)^2$, $k=0,1,2,\ldots$. Since all $\Lambda_{n,k}$ are real and nonnegative, then if there are no multiple eigenvalues in this spectrum, the small amplitude nonlinear modes are *linearly stable* for both repulsive and attractive nonlinearities. However, if the spectrum of $\mathcal{L}_n^2$ includes multiple eigenvalues the stability analysis implies the study of splitting of these eigenvalues when passing from $\varepsilon=0$ to $0<\varepsilon\ll 1$ (see, e.g., [26,27]).

F. Krein signature

Let n be fixed and a pair $(\Lambda,\zeta(x))$ be a solution of eigenvalue problem (18) where $\Lambda>0$ is a semisimple eigenvalue of $L_n^- L_n^+$ and the corresponding eigenfunction $\zeta(x)$ is real. It is useful to assign to any such pair $(\Lambda,\zeta(x))$ the value

$$K = \mathrm{sign}\langle L_n^+\zeta(x),\zeta(x)\rangle$$

called the *Krein signature* [28]. As the solution $\psi_n(x)$ of Eq. (6) varies along the branch Γ_n together with ω_n, the eigenvalues of the operator $L_n^+ L_n^-$ also vary, but the Krein signature of any pair $(\Lambda,\zeta(x))$ is conserved while there is no collision between eigenvalues. When a collision between a pair of real positive eigenvalues takes place, they can become complex *only* in the case when their Krein signatures are opposite; otherwise these eigenvalues pass through each other both remaining real. So, as ω_n varies along the branch Γ_n the interactions of eigenvalues with opposite Krein signatures may affect the stability of modes in this branch.

The inverse statement is also valid but *in a generic situation* only [28]: if the Krein signatures of colliding eigenvalues are opposite then *generically* after collision they become complex. However, additional symmetries of the solution can destroy this picture: it will be shown that in some cases eigenvalues with opposite Krein signatures can also pass through each other without causing instabilities.

III. RESULTS FOR THE HARMONIC POTENTIAL $V(x)=x^2$

A. General comments

In the case of the harmonic oscillator, where $V(x)=x^2$, the branches Γ_n, $n=0,1,2,\ldots$ are depicted in Figs. 1(a) and 1(b). It follows from Fig. 1 that the branches Γ_n are represented by monotonic (at least for moderate values of N, ω, and n) functions $N(\omega)$. Previous numerical results [11] allow one to conjecture that there are no solutions without a linear counterpart for this potential. It is known that the solutions corresponding to the branches Γ_0 and Γ_1 in both attractive and repulsive cases are stable (see, for instance, [10–12] for more detailed analyses of perturbed solutions from Γ_1). Numerical calculations show that the modes from $\Gamma_2^{(r)}$ (the repulsive

TABLE I. Eigenvalues of $\mathcal{L}_{1,2}$ and $\mathcal{L}_{1,2}^2$. The boxes are used to emphasize the doubles eigenvalues.

Eigenfrequency number	Zeroth $\tilde{\psi}_0(x)$	First $\tilde{\psi}_1(x)$	Second $\tilde{\psi}_2(x)$	Third $\tilde{\psi}_3(x)$	Fourth $\tilde{\psi}_4(x)$	Fifth $\tilde{\psi}_5(x)$
$\mathcal{L}_1$	2	0	−2	−4	−6	−8
$\mathcal{L}_1^2$	$\boxed{4}$	0	$\boxed{4}$	16	36	64
$\mathcal{L}_2$	4	2	0	−2	−4	−6
$\mathcal{L}_2^2$	$\boxed{16}$	$\boxed{4}$	0	$\boxed{4}$	$\boxed{16}$	36

case) are unstable. In the attractive case the family $\Gamma_2^{(a)}$ corresponds to unstable modes for ω close to the bifurcation point $\omega_2=5$. More specifically, in Ref. [11] the instability has been observed for $\omega^*<\omega<5$ where $\omega^*\approx 3.83$. It has also been found that for $\omega<\omega^*$ the mode is stable.

B. Small-amplitude modes

Let us now analyze the stability of the branch Γ_n for both attractive and repulsive cases when ω_n lies close to the bifurcation point $\tilde{\omega}_n$. In the bifurcation point (linear limit) the solutions of the eigenvalue problem (7) are the pairs $(\tilde{\omega}_n, \tilde{\psi}_n(x))$, $n=0,1,\ldots$ where

$$\tilde{\omega}_n = 2n+1, \tag{23a}$$

$$\tilde{\psi}_n(x) = \frac{1}{\sqrt{2^n n!\sqrt{\pi}}} H_n(x) e^{-1/2x^2}, \tag{23b}$$

and $H_n(x)$ is nth Hermite polynomial (see, e.g., [25]).

The stability of small amplitude solutions can be studied using formulas (18)–(22). Let us start with the case $\varepsilon=0$. The spectrum of the operator $\mathcal{L}_n$ is equidistant and consists of the eigenvalues $\lambda_{n,k}=2(n-k)$ and the corresponding eigenfunctions are given by $\tilde{\psi}_k(x)$, $k=0,1,\ldots$. All the eigenvalues are simple and there is one zero eigenvalue. The eigenvalues of the operator $\mathcal{L}_n^2$ are $\Lambda_{n,k}=\lambda_{n,k}^2=4(k-n)^2$ and they correspond to the same eigenfunctions $\tilde{\psi}_k(x)$, $k=0,1,\ldots$. This means that the spectrum of $\mathcal{L}_n^2$ includes n *double eigenvalues* $\Lambda_{n,k}=4(n-k)^2$, $k=0,1,\ldots(n-1)$, one *simple zero eigenvalue* and *infinitely many simple positive eigenvalues*. The mechanism of emerging of double eigenvalues becomes transparent from Table I. Each of the double eigenvalues $\Lambda_{n,k}$ has an invariant subspace spanned by two functions, $\tilde{\psi}_k(x)$ and $\tilde{\psi}_{2n-k}(x)$.

Following Ref. [27] we consider the 2×2 matrices

$$\tilde{M}_{n,k} = \begin{pmatrix} \langle M_n\tilde{\psi}_k, \tilde{\psi}_k\rangle & \langle M_n\tilde{\psi}_k, \tilde{\psi}_{2n-k}\rangle \\ \langle M_n\tilde{\psi}_{2n-k}, \tilde{\psi}_k\rangle & \langle M_n\tilde{\psi}_{2n-k}, \tilde{\psi}_{2n-k}\rangle \end{pmatrix}.$$

If the eigenvalues of $\tilde{M}_{n,k}$ are $\mu_{n,k}^{(1)}$ and $\mu_{n,k}^{(2)}$, $\mu_{n,k}^{(1)}\neq\mu_{n,k}^{(2)}$, then for $\varepsilon\ll 1$ the double eigenvalue $\Lambda_{n,k}$ of $\mathcal{L}_n^2$ splits into two simple eigenvalues of $L_n^- L_n^+$: $\Lambda_{n,k}^{(j)}=\Lambda_{n,k}+\varepsilon^2\sigma\mu_{n,k}^{(j)}+o(\varepsilon^2)$ where $j=1,2$. Therefore if the eigenvalues of any of the matrices $\tilde{M}_{n,k}$, $k=0,\ldots,n-1$ are complex, the instability of the small-amplitude solution $\Psi(t,x)=e^{-i\omega_n t}\psi_n(x)$ takes place. It is important that since both repulsive ($\sigma=-1$) and attractive ($\sigma=1$) cases are described by the eigenvalues of the same matrices $\tilde{M}_{n,k}$, the complex eigenvalues of $\tilde{M}_{n,k}$ for some k means the instability of small-amplitude modes in both repulsive and attractive cases.

Simple but tedious algebra gives the expressions for the elements of the matrices $\tilde{M}_{n,k}$:

$$\langle M_n\tilde{\psi}_k, \tilde{\psi}_k\rangle = \frac{8(n-k)}{\pi 2^{(n+k)} n!\, k!}\int_{-\infty}^{\infty} H_n^2(x)H_k^2(x)e^{-2x^2}dx - \frac{4(n-k)}{\pi 2^{2n}(n!)^2}\int_{-\infty}^{\infty} H_n^4(x)e^{-2x^2}dx,$$

$$\langle M_n\tilde{\psi}_k, \tilde{\psi}_{2n-k}\rangle = -\langle M_n\tilde{\psi}_{2n-k}, \tilde{\psi}_k\rangle = \frac{4(n-k)}{\pi 2^{2n} n!\sqrt{k!\,(2n-k)!}} \times \int_{-\infty}^{\infty} H_n^2(x)H_{2n-k}(x)H_k(x)e^{-2x^2}dx,$$

$$\langle M_n\tilde{\psi}_{2n-k}, \tilde{\psi}_{2n-k}\rangle = -\frac{8(n-k)}{\pi 2^{(3n-k)} n!\,(2n-k)!}\int_{-\infty}^{\infty} H_n^2(x)H_{2n-k}^2(x)e^{-2x^2}dx + \frac{4(n-k)}{\pi 2^{2n}(n!)^2}\int_{-\infty}^{\infty} H_n^4(x)e^{-2x^2}dx.$$

Using MAPLE we calculated the eigenvalues of the matrix $\tilde{M}_{n,k}$. The results are collected in Table II where we observe the following facts.

(i) In columns 2–6 there is at least one letter "C" which means instability of small-amplitude modes belonging to the respective branch Γ_n, for both attractive and repulsive nonlinearities. We conjecture that the instability of small-amplitude modes takes place for all branches $\Gamma_n^{(a)}$ and $\Gamma_n^{(r)}$ with $n\geq 2$.

(ii) In the case $n=1$ the mode is stable. That confirms the results of [10] (see Fig. 1 there). It is interesting that in the limit $\varepsilon=0$ the algebraic and geometric multiplicities of the eigenvalue $\Lambda=4$ are both equal to 2. At the same time two real eigenvalues emerging from the double eigenvalue $\Lambda=4$ for $\varepsilon\ll 1$ have opposite Krein signatures which do not correspond to the generic case (see [28]).

TABLE II. Eigenvalues of the matrices $\tilde{M}_{n,k}$. Each cell of the table for $n>k$ contains either the letter "C," meaning that the eigenvalues are complex, or two real eigenvalues.

	$n=1$	$n=2$	$n=3$	$n=4$	$n=5$	$n=6$
$k=0$	0.199	C	C	0.133	−0.005	−0.135
	0			0.404	0.618	0.816
$k=1$	–	0.125	C	C	C	0.058
		0				0.473
$k=2$	–	–	0.089	C	C	C
			0			
$k=3$	–	–	–	0.068	C	C
				0		
$k=4$	–	–	–	–	0.055	C
					0	
$k=5$	–	–	–	–	–	0.045
						0

(iii) When $n=k+1$ the matrix $\tilde{M}_{n,k}$ has a zero eigenvalue. This reflects the fact that

$$\zeta(x) = \frac{d\psi_n(x)}{dx} \tag{24}$$

is an eigenfunction of the operator $L_n^- L_n^+$ corresponding to $\Lambda=4$ for *any* mode $\psi_n(x)$ belonging to any branch $\Gamma_n^{(a)}$ or $\Gamma_n^{(r)}$.

C. Nonlinear modes of arbitrary amplitudes

In order to study the linear stability of the nonlinear modes of a finite amplitude we have first calculated the modes using a modified shooting method developed in Ref. [11] and used in Refs. [11,29] to compute different families of nonlinear modes. Then we have found numerically the eigenvalues of the operator $L_n^- L_n^+$. To do so we have approximated the solution $\psi_n(x)$ on a grid, replacing the second derivatives in $L_n^{\pm}$ by second-order finite differences and calculated the eigenvalues of the resulting sparse matrix. The result is shown in Figs. 2 and 3. One can see that the families $\Gamma_2^{(a,r)}$ at $\omega=5$ possess two double eigenvalues [Figs. 2(b), 2(c), 2(e), and 2(f)], $\Lambda=4$ (merged eigenvalues $\Lambda_{2,1}=\Lambda_{2,3}$) and $\Lambda=16$ (merged eigenvalues $\Lambda_{2,0}=\Lambda_{2,4}$). These eigenvalues split; in the case of $\Lambda=4$ the resulting eigenvalues remain real and positive, one of them corresponding to the exact solution ((24)). In the case of $\Lambda=16$, if the nonlinearity is attractive, there exist two complex eigenvalues on the interval $\omega^*<\omega<5$, $\omega^*\approx 3.83$. At $\omega=\omega^*$ these eigenvalues merge and the mode becomes stable. Since the number of particles N of the mode grows when moving along the branch Γ_2, one can say that there is a *threshold on the number of particles* for the stability of the mode in attractive case. If the nonlinearity is repulsive, the two complex eigenvalues do not disappear through all the regions of parameter ω investigated; therefore the mode remains unstable. In the case of the family Γ_3 [Figs. 3(a)–3(f)] at $\omega=7$ there are three double eigenvalues $\Lambda=4$, 16, and 36 which split. Then the scenario is similar to the case of the family Γ_2. The eigenvalues originated by $\Lambda=4$ remain real and one of them corresponds to the exact solution (24). In the attractive case the mode becomes stable after the two pairs of eigenvalues merge, i.e., for $\omega\lesssim -2.10$; at this point the second pair of the eigenvalues (both originated from $\Lambda=36$) merges. In the repulsive case the mode remains unstable through all the regions of the parameter ω studied.

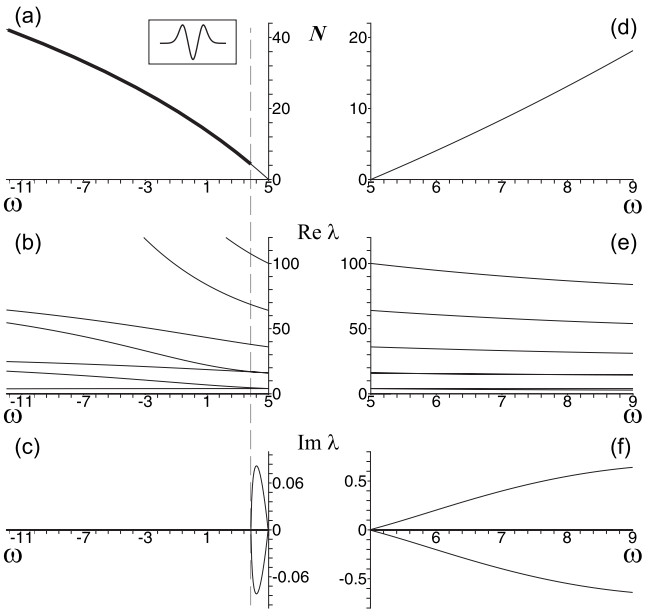

FIG. 2. Branches $\Gamma_n^{(a,r)}$ and plots of real and imaginary parts of eigenvalues Λ of the operator $L_n^- L_n^+$ vs ω for $V(x)=x^2$ and $n=2$. (a) N vs ω for the branch $\Gamma_2^{(a)}$ (the part of the branch corresponding to stable solutions is shown in bold). (b) Real and (c) imaginary parts of the eigenvalues Λ for the attractive case. The splitting of the lowest eigenvalues $\Lambda=4$ and 16 of the linear problem is highlighted by the vertical dashed line. The nonzero imaginary part in panel (c) corresponds to the eigenvalues originated by $\Lambda=16$ of the linear problem for $\omega^*<\omega<5$ (see the text). Plots (d)–(f) are analogous to (a)–(c) but for the repulsive case. The branch studied is $\Gamma_2^{(r)}$ and the eigenvalues originated by $\Lambda=16$ remain complex for the whole interval of ω studied [see panel (f)], and therefore the mode is unstable.

Summarizing, our results support that high-order modes of GPE with harmonic potential and attractive interactions are stable when the number of particles exceeds a threshold value (different for each branch), which corroborates our analysis on the quasilinear behavior of upper modes made in the beginning of Sec. II C. In the repulsive case, high-order modes of GPE with a harmonic potential are unstable. Our result contradict those of [13] where it was claimed that stable modes exist for both signs of the nonlinear term.

IV. ANHARMONIC POTENTIALS (I): SMALL PERTURBATIONS OF A HARMONIC POTENTIAL

Now we turn our attention to the GPE with a harmonic potential perturbed by a quartic term, $V(x)=x^2+\kappa x^4$, $0<|\kappa|\ll 1$. In this case the eigenvalues $\tilde{\omega}_n$ and eigenfunctions $\tilde{\psi}_n(x)$, $n=0,1,\ldots$, for the linear problem (7) can be found

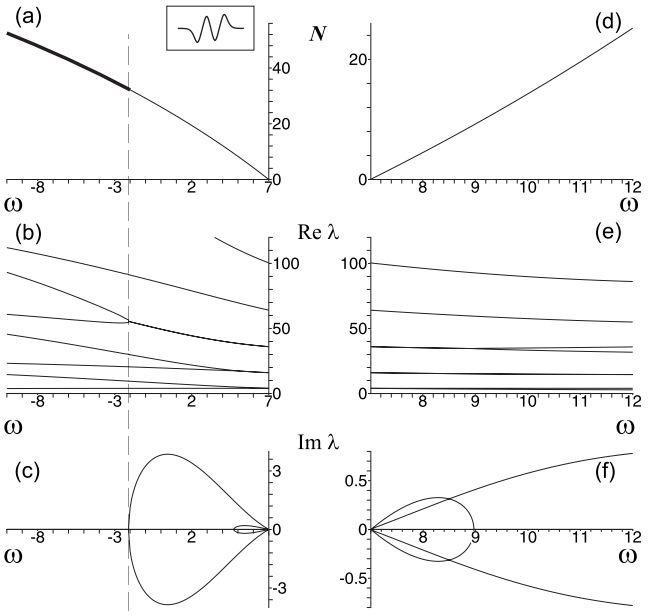

FIG. 3. Branches $\Gamma_n^{(a,r)}$ and plots of the real and imaginary parts of the eigenvalues Λ vs ω for the potential $V(x)=x^2$ and $n=3$. All the plots are organized in the same way as in Fig. 2.

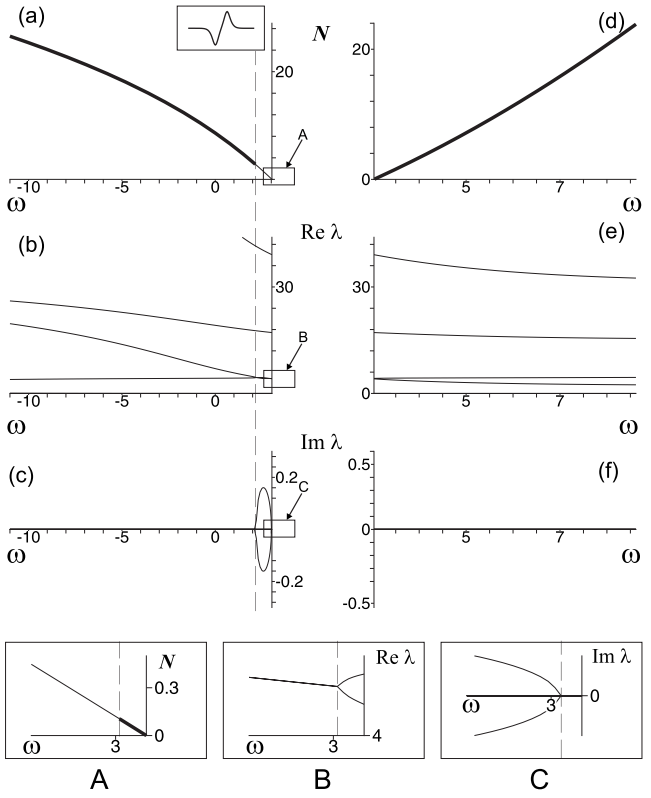

FIG. 4. Branches $\Gamma_n^{(a,r)}$ and plots of the real and imaginary parts of eigenvalues Λ of the operator $L_n^- L_n^+$ vsω for $V(x)=x^2+0.01x^4$ and $n=1$. Plots (a)–(f) are organized as in Fig. 2. In the attractive case the dashed line on the plots (a)–(c) marks the upper boundary of the instability window. The lower boundary of this instability window is very close to $N=0$, and not visible on the scale of the plots (a)–(f). Plots (A)–(C) show the branch $\Gamma_1^{(a)}$ and the real and imaginary parts of eigenvalues $\Lambda_{1,0}$ and $\Lambda_{1,2}$ vs ω close to the linear limit $\omega=\tilde{\omega}_1$ (i.e., $N=0$) with magnification. In the plots (A)–(C) the lower boundary of the instability window is marked with a dashed line.

numerically or by means of asymptotic procedures [30]. Also one has to employ numerics for the construction of the branches of nonlinear modes $\Gamma_n^{(a)}$ and $\Gamma_n^{(r)}$; which are similar to the corresponding branches for the harmonic potential case except for small deformations. As in the purely harmonic case, the branches $\Gamma_n^{(a,r)}$ are monotonic (at least for moderate values of N, ω, and n) and can be parametrized by any of the parameters N and ω. However, the spectrum $\tilde{\omega}_n$ is no longer equidistant, which has several important consequences as we will discuss in what follows.

A. Small amplitude modes

The stability of small amplitude modes belonging to the branches $\Gamma_n^{(a,r)}$ in the case of the anharmonic potential can be also studied by means of asymptotic expansions (18)–(22). Consider the case $\varepsilon=0$. The spectrum of the operator $\mathcal{L}_n^2$ now consists of simple eigenvalues $\Lambda_{n,k}=(\tilde{\omega}_k-\tilde{\omega}_n)^2$, $k=0,1,\ldots$, and the Krein signature of the eigenvalue $\Lambda_{n,k}$ is $K_{n,k}=\mathrm{sign}(n-k)$. Therefore if κ is small the spectrum of $\mathcal{L}_n^2$ contains n pairs of close eigenvalues of opposite Krein signatures, $\Lambda_{n,k}$ and $\Lambda_{n,2n-k}$, $k=0,1,\ldots,n-1$, which are, nevertheless, different. The spectrum contains also a zero eigenvalue and an infinite sequence of increasing positive eigenvalues. Therefore, generally speaking, the spectrum $\Lambda_{n,k}$, $k=0,1,\ldots$ does not contain multiple eigenvalues.

When passing from $\varepsilon=0$ to $0<\varepsilon\ll 1$ the eigenvalues $\Lambda_{n,k}$ of the operator $L_n^- L_n^+$ vary continuously. Therefore one can expect the stability of the mode until two eigenvalues with opposite Krein signature merge. So, the small amplitude modes are expected to be stable for all the branches $\Gamma_n^{(a)}$ and $\Gamma_n^{(r)}$.

B. Nonlinear modes of arbitrary amplitude: $\kappa>0$

In order to study the linear stability of the nonlinear modes of a finite amplitude we have first calculated the spectrum of the operator $L_n^- L_n^+$ numerically, concentrating on the branches $\Gamma_n^{(a,r)}$ for $n=0,1,\ldots,4$. The obtained general picture appears to be very different from that of the harmonic potential. The plots of real and imaginary parts of the eigenvalues Λ vs ω for the branches Γ_1, Γ_2, and Γ_3 in both attractive and repulsive cases are shown in Figs. 4–6.

The *general property* of all the cases considered is that the instability of the nonlinear modes occurs *only* due to collisions of pairs of eigenvalues which are a continuation of the respective eigenvalues $\Lambda_{n,k}$ and $\Lambda_{n,2n-k}$ in the linear limit, i.e., of the eigenvalues of the operator $\mathcal{L}_n^2$. In what follows we call them $(\Lambda_{n,k},\Lambda_{n,2n-k})$ *-pairs*. The eigenvalues in these pairs have opposite Krein signatures.

Then, the other numerical results can be structured as follows.

a. Repulsive nonlinearity. The ground state modes corresponding to the branch $\Gamma_0^{(r)}$ are stable since there are no $(\Lambda_{n,k},\Lambda_{n,2n-k})$-pairs in the spectrum of $L_0^- L_0^+$. The modes from the next branch, $\Gamma_1^{(r)}$, in the limit of strong nonlinearity correspond to "dark" soliton modes; there is one $(\Lambda_{n,k},\Lambda_{n,2n-k})$-pair in the spectrum of $L_1^- L_1^+$, but no collisions

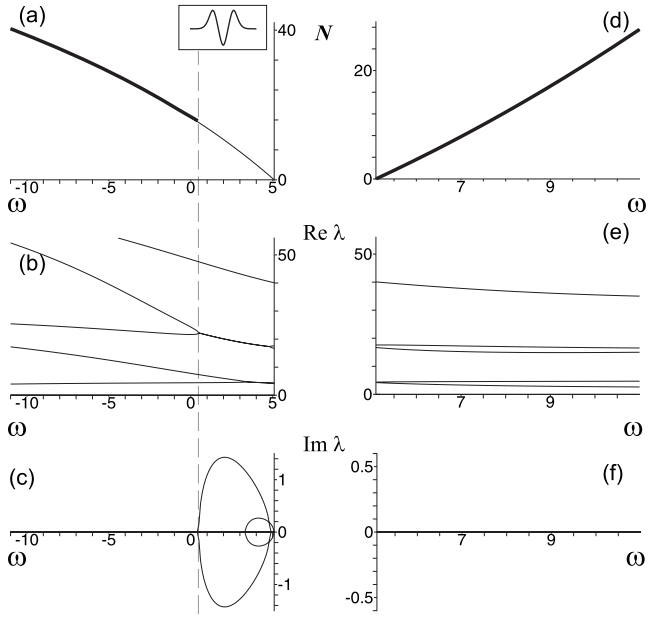

FIG. 5. Branches $\Gamma_n^{(a,r)}$ and plots of the real and imaginary parts of eigenvalues Λ of the operator $L_n^- L_n^+$ vs ω for $V(x)=x^2+0.01x^4$ and $n=2$. In the attractive case the lower boundary is very close to $N=0$ and not visible on the scale of the figure. All the plots are organized as in Fig. 2.

of eigenvalues have been found when tracing the modes of this branch within the range of parameter N where it has been investigated (see Fig. 4, right panels). Therefore we conclude that the modes from $\Gamma_1^{(r)}$ are *stable*. A similar situation takes place for the branch $\Gamma_2^{(r)}$ where two $(\Lambda_{n,k},\Lambda_{n,2n-k})$-pairs in the spectrum of $L_2^- L_2^+$ are present: no

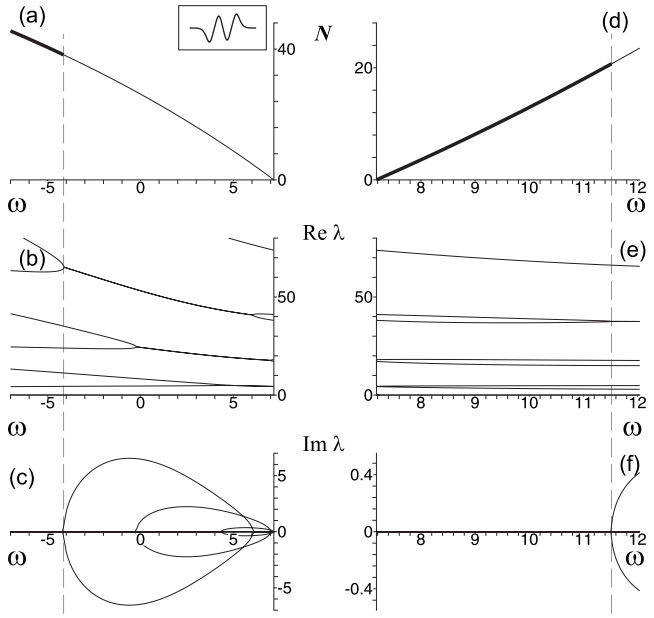

FIG. 6. Branches $\Gamma_n^{(a,r)}$ and plots of the real and imaginary parts of eigenvalues Λ of the operator $L_n^- L_n^+$ vs ω for $V(x)=x^2+0.01x^4$ and $n=3$. In the attractive case the lower boundary is very close to $N=0$, and not visible on the scale of the figure. All the plots are organized as in Fig. 2.

collision has been observed within the range of parameter N under consideration (see Fig. 5, right panels). However, this is not the case for higher branches. For instance, the collisions of eigenvalues have been observed for nonlinear modes from $\Gamma_3^{(r)}$. The spectrum of the operator $L_3^- L_3^+$ includes three $(\Lambda_{n,k},\Lambda_{n,2n-k})$-pair and a collision of one of them (highest) at some large enough value of N has been seen (see Fig. 5, right panels). After the point of collision (i.e., for greater values of N) the pair of collided eigenvalues become complex which means the instability of corresponding nonlinear modes. A similar situation takes place for the branch $\Gamma_4^{(r)}$. In general, this points to the fact that the instability of higher modes, generically, takes place, if the number of particles N exceed some threshold value, which is particular for each branch $\Gamma_n^{(r)}$. The existence of the threshold value for the branches $\Gamma_1^{(r)}$ and $\Gamma_2^{(r)}$ which we have not found in our numerical investigation needs more delicate analysis.

b. Attractive nonlinearity. The ground state modes of the branch $\Gamma_0^{(a)}$ are stable. For the branch $\Gamma_1^{(a)}$, there is one $(\Lambda_{n,k},\Lambda_{n,2n-k})$-pair in the spectrum of $L_1^- L_1^+$ (see Fig. 4, left panels). Then there exist two bifurcation values of the parameter N (the number of particles). When N, increasing, reaches the first bifurcation value, the eigenvalues of this pair collide and become complex. For the values of N below this threshold, the mode is stable; however, for the potential under consideration the first bifurcation value is very tiny, so it is not visible in Fig. 4. Then, when N reaches the second bifurcation value, the complex eigenvalue collides again and becomes real. So, we can conclude that the modes of $\Gamma_1^{(a)}$ are *stable* unless the number of particles N belongs to an *instability window*; the lower bound of this window is close to zero (but separated from zero). The size of the window of instability increases when κ grows and both bounds of this window are quite sensitive to the variation of κ. A similar situation has been observed for higher branches of nonlinear modes. For instance, the spectrum of the operator spectrum of $L_2^- L_2^+$, the branch $\Gamma_2^{(a)}$, includes two $(\Lambda_{n,k},\Lambda_{n,2n-k})$-pairs. As N grows both of them undergo the same evolution: they become complex at the first bifurcation value of N and return to be real at the second bifurcation value (see Fig. 5, left panels). The interval with respect to N between the first bifurcation value for the pair $(\Lambda_{2,1},\Lambda_{2,3})$ and second bifurcation value for the pair $(\Lambda_{2,0},\Lambda_{2,4})$ represents *the window of instability*. The upper boundary of this instability window is marked by a dashed line in Fig. 5. However, since the first bifurcation value for the pair $(\Lambda_{2,1},\Lambda_{2,3})$ [lowest curve in Fig. 5(b)] is very tiny, the lower boundary of the instability window cannot be separate from zero in Fig. 5. Therefore the modes from $\Gamma_2^{(a)}$ are stable if N does not belong to the instability window. This situation, probably, is generic for other higher branches.

To confirm our results on the stability of nonlinear high-order modes we also have performed a series of direct numerical simulations of their evolution, perturbed by a random perturbation of 5% amplitude of the mode. Thus we have simulated the evolution of initial data of the form $\psi_0(x)=\psi_n(x)[1+r(x)]$ with $r(x)$ a white noise of maximum amplitude 0.05. The subsequent dynamics of the modes under Eq. (5) was computed using a second order in time split-step pseudospectral scheme discretized in space using trigo-

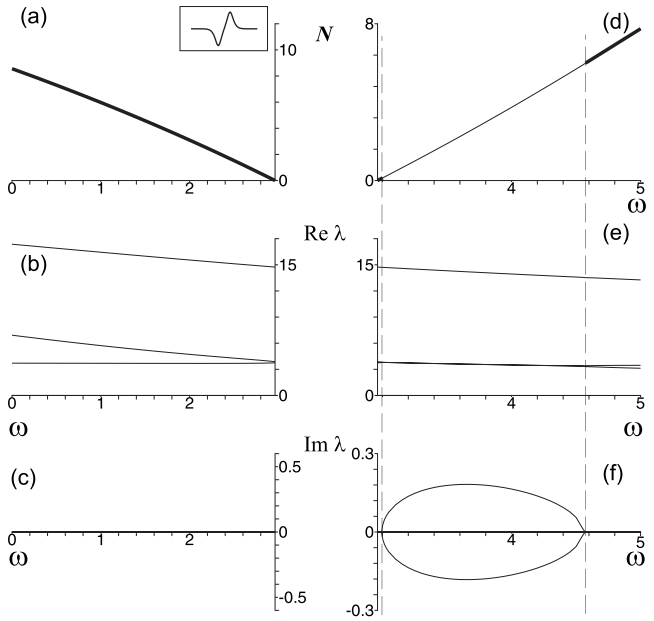

FIG. 7. Branches $\Gamma_n^{(a,r)}$ and plots of the real and imaginary parts of eigenvalues Λ of the operator $L_n^- L_n^+$ vs ω for $V(x)=x^2-0.01x^4$ and $n=1$. All the plots are organized as in Fig. 2.

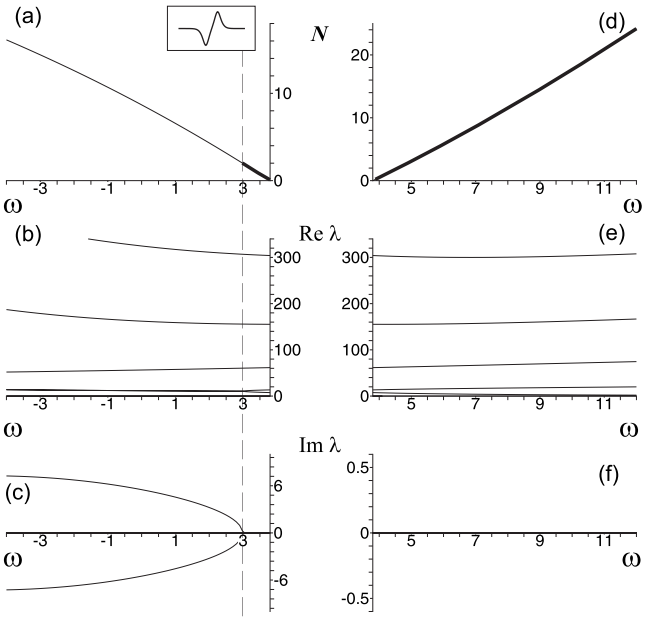

FIG. 8. Branches $\Gamma_n^{(a,r)}$ and the plots of the real and imaginary parts of eigenvalues Λ of the operator $L_n^- L_n^+$ vs ω for $V(x)=x^4$ and $n=1$. All the plots are organized in the same manner as in Fig. 2.

nometric polynomials (via the fast Fourier transform). In all the cases studied, which included most of the branches presented here our test verified the predictions based on linear stability analysis.

C. Nonlinear modes of arbitrary amplitude: $\kappa<0$

Let us briefly summarize the stability results for the potential $V(x)=x^2+\kappa x^4$, $0<|\kappa|\ll 1$ and $\kappa<0$. In this case only a *finite* number of branches $\Gamma_n^{(a,r)}$ can exist, since there is a finite number of discrete eigenvalues for Eq. (7). These branches can be found numerically. The linear stability analysis performed for the potential $V(x)=x^2-0.01x^4$ shows (see Fig. 7) that all solutions of the branch $\Gamma_1^{(a)}$ which we have considered are linearly stable. On the other hand, the modes of $\Gamma_1^{(r)}$ are also stable, except some instability window situated close to the point of branching. This is in contrast with the case $\kappa>0$, since in that case the instability window is situated on the branch $\Gamma_1^{(a)}$ but not $\Gamma_1^{(r)}$. The solutions of the branch $\Gamma_2^{(a)}$ are also linearly stable whereas the solutions of the branch $\Gamma_2^{(r)}$ are stable only in the vicinity of the branching point, i.e., only for $N\ll 1$. For the branches $\Gamma_3^{(a,r)}$ the picture of stability-instability becomes more complex.

V. ANHARMONIC POTENTIALS (II): POTENTIAL $V(x)=x^4$

In order to show that the results for anharmonic potentials are quite generic, let us consider a GPE with $V(x)=x^4$. Again, the eigenvalues, $\tilde{\omega}_n$, and eigenfunctions $\tilde{\psi}_n(x)$, $n=0,1,\ldots$, for the linear problem (7) cannot be obtained exactly. The branches of nonlinear modes $\Gamma_n^{(a)}$ and $\Gamma_n^{(r)}$ which have been found numerically for $n=0,1,2,3$ are similar to the corresponding branches for the harmonic potential case. These branches are monotonic (at least for moderate values of N, ω, and n) and can be parametrized by any of the parameters N, ω.

Due to the reasons discussed above, the small amplitude solutions of GPE with the potential $V(x)=x^4$ generically *are stable* for both attractive and repulsive nonlinearities. In order to study the stability of nonlinear modes in general, we have analyzed the bifurcations of eigenvalues of $L_n^- L_n^+$ when $\psi_n(x)$ varies along the families $\Gamma_n^{(a)}$ and $\Gamma_n^{(r)}$. Our numerical investigation shows that, as in the case of weak anharmonicity, the instability of nonlinear modes from Γ_n occurs *only* due to collisions of those pairs of eigenvalues which are a continuation of eigenvalues $\Lambda_{n,k}$ and $\Lambda_{n,2n-k}$ in the linear limit, i.e., in the spectrum of $\mathcal{L}_n^2$. These eigenvalues $\Lambda_{n,k}$ and $\Lambda_{n,2n-k}$ are of opposite Krein signature. Again, let us refer to these pairs of eigenvalues as $(\Lambda_{n,k},\Lambda_{n,2n-k})$-pairs.

Qualitatively, the stability picture for the case $V(x)=x^4$ is the same as in the case $V(x)=x^2+\kappa x^4$, $\kappa>0$, except for some minor differences. The first one is that we have not found the threshold of instability in N in the case of repulsive nonlinearity for the modes in the branches $\Gamma_n^{(r)}$, $n=0,1,2,3$. Therefore these modes are stable in all of the parameter range studied. Second, we have not found an upper bound of the instability window in N in the case of attractive nonlinearity for the modes from $\Gamma_n^{(a)}$, $n=1,2,3$. We believe that it is a technical problem related to the finiteness of the region studied but we think an upper bound of this instability window exists. The plots of real and imaginary parts of eigenvalues Λ of the operator $L_n^- L_n^+$ versus ω for the branches Γ_1, Γ_2, and Γ_3 for attractive and repulsive nonlinearities are shown in Figs. 8–10.

It is interesting to mention that we have also observed collisions of eigenvalues with opposite Krein signatures which belong to different $(\Lambda_{n,k},\Lambda_{n,2n-k})$-pairs. In our case they did not lead to instability since they remained real after

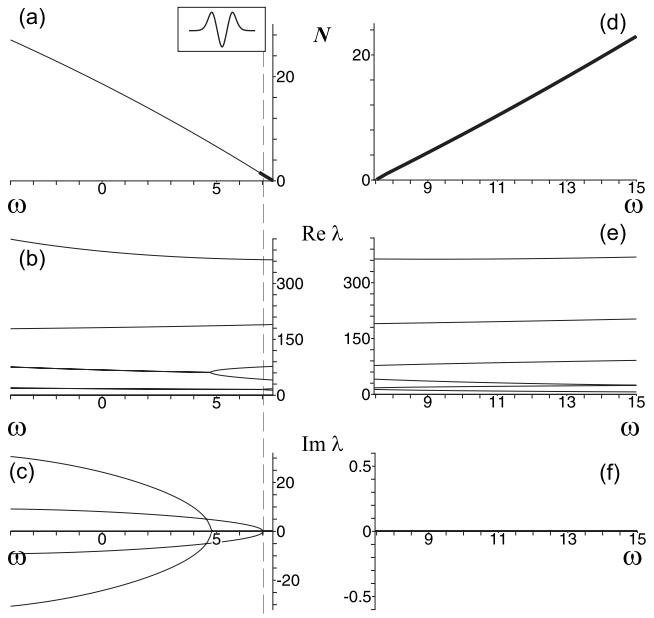

FIG. 9. Branches $\Gamma_n^{(a,r)}$ and the plots of the real and imaginary parts of eigenvalues Λ of the operator $L_n^- L_n^+$ vs ω for $V(x)=x^4$ and $n=2$. All the plots are organized in the same manner as in Fig. 2.

the collision [see, for example, Fig. 10(e)]. This phenomenon does not correspond to a generic situation; it is caused by the opposite parity of colliding eigenfunctions (one of them was odd, while the other one was even).

We have also performed a set of direct numerical simulations of the evolution of perturbed stationary modes in Eq. (5) as described in Sec. IV B. The outcome of those

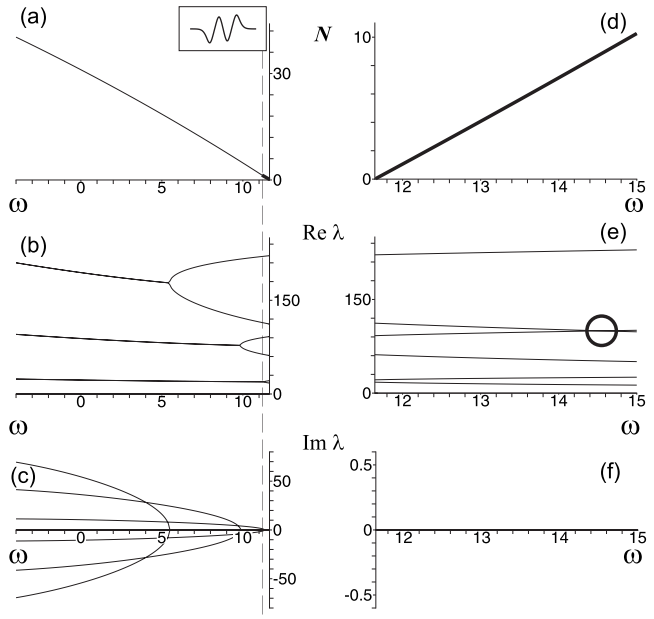

FIG. 10. Branches $\Gamma_n^{(a,r)}$ and the plots of the real and imaginary parts of eigenvalues Λ of the operator $L_n^- L_n^+$ vs ω for $V(x)=x^4$ and $n=3$. All the plots are organized in the same manner as in Fig. 2. The bold circle in the plot (e) highlights the collision of the eigenvalues of opposite Krein signatures which does not lead to instability.

simulations confirms the results of the linear stability analysis.

VI. CONCLUSIONS AND DISCUSSION

Using a combination of different analytical and numerical tools including the analysis of the small amplitude limit, the nonlinear WKB approximation, the Krein signature, and direct numerical simulations we have analyzed the stability properties of higher-order nonlinear trapped modes for the GPE with different potentials. First, we have reviewed the results for the harmonic potential $V(x)=x^2$ and discussed how the stability of the modes is essentially affected by the fact that levels are equidistant. Next, we have considered the weakly anharmonic potential $V(x)=x^2+\kappa x^4$, $0<|\kappa|\ll 1$. Our results, summarized in Table III, lead to the conclusion that even a small anharmonicity which does not affect essentially the shape of the modes, improves drastically the stability properties of higher-order modes due to the fact that none of these potentials has an equidistant spectrum. We conjecture that the same situation would take place also for a more generic perturbation of the harmonic potential, for instance, by nonsymmetric (e.g., cubic) perturbation.

Then we have checked that in the case of stronger anharmonicity $V(x)=x^4$ the stability-instability picture is similar to the case of potential $V(x)=x^2+\kappa x^4$, $0<\kappa\ll 1$, $\kappa>0$. We have studied the GPE with the potential $V(x)=x^6$ (the details have not been discussed in this paper) and found that they reproduce the same essential features.

It follows from the arguments presented that the scenario for the appearance of instability induced by the equidistant spectrum of the harmonic oscillator holds also for other classes of potentials with equidistant spectra (for construction of such potentials see [32–34]) or, more generally, for potentials for which the spacing between some levels (not necessarily adjacent) are equal. In that situation, the splitting of double eigenvalues for the operator $\mathcal{L}_n^2$ can lead to complex eigenvalues in the linear stability problem.

An interesting point for further investigation is the effect of the type of confining potential on the stability of higher order modes in two spatial dimensions, e.g., the stability of vortices under deformations of the potential. This subject has attracted a lot of attention in the last years [14–22] and the methodology developed in this paper could be useful. In fact, the situation is similar to the one considered above. In the case of harmonic potentials the spectrum of the corresponding eigenvalue problem is equidistant; the corresponding eigenfunctions are Gauss-Laguerre modes. Then, one can expect that switching to anharmonic potentials can also change the stability properties of vortices and other higher order modes.

Finally, we would like to mention another practical implication of the enhanced stability of nonlinear modes by the anharmonicity of the trap potential. As it was suggested in [10] such modes can grow from the eigenstates of the linear oscillator by increasing the nonlinearity using Feshbach resonance management (in the language of this paper this corresponds to the "motion" along a nonlinear branch starting

TABLE III. Comparison of the stability properties for the potentials $V(x)=x^2$, $V(x)=x^2+\kappa x^4$ (for $\kappa>0$), and $V(x)=x^4$. The results for $\kappa<0$ are not included in this table but are discussed in the text

	$V(x)=x^2$	$V(x)=x^2+\kappa x^4,\ \kappa>0$	$V(x)=x^4$
Zeroth mode (ground state), $\sigma=\pm 1$	**Stable**	**Stable**	**Stable**
First mode, $\sigma=1$, small amplitude limit	**Stable**	**Stable**	**Stable**
First mode ("bright soliton"), $\sigma=1$, general case	**Stable**	**Unstable**, if N belongs to some "instability window." The lower bound of this "window" is separated from zero. The size of the "window" grows with κ. Otherwise **stable**.	**Unstable**, if N belongs to some "instability window," with lower bound separated from zero. Otherwise **stable**.
First mode, $\sigma=-1$, small amplitude limit	**Stable**	**Stable**	**Stable**
First mode ("dark soliton") $\sigma=-1$, general case	**Stable**	**Stable** for all N which have been considered.	**Stable** for all N which have been considered.
Higher modes, $\sigma=1$, small amplitude limit	**Unstable**	**Stable**	**Stable**
Higher modes, $\sigma=1$, general case	**Stable**, if N exceeds a threshold.	**Unstable**, if N belongs to some "instability window," with lower bound separated from zero. The size of the "window" grows with N. Otherwise **stable**.	*Hypothetically,* **unstable**, if N lies in a large "window" of instability. The upper boundary of this "window" has not been found in our numerics.
Higher modes, $\sigma=-1$, small amplitude limit	**Unstable**	**Stable**	**Stable**
Higher modes, $\sigma=-1$, general case	**Unstable**	*Hypothetically* **unstable**, if N exceeds some threshold. Otherwise **stable**.	**Stable** for all N which we have considered.

from the bifurcation point as the number of particles increases starting from zero). This fact can be used for the generation of single solitons or even solitonic trains. The instability of the nonlinear modes in the case of the harmonic potential was the major obstacle for the practical implementation of that mechanism. However, the idea becomes experimentally feasible if an anharmoic potential is used since now higher order branches have a different stability and thus can lead to stable solitons.

ACKNOWLEDGMENTS

G.A. acknowledges the support from the President Program for Leading Scientific Schools (Project No. 3826.2008.2). The work of V.V.K. was supported by Grant No. POCI/FIS/56237/2004 (European Program FEDER and FCT, Portugal). V.M.P.G. was partially supported by Grants No. FIS2006-04190 (Ministerio de Educación y Ciencia, Spain) and No. PCI-08-0093 (Junta de Comunidades de Castilla-La Mancha, Spain).

[1] C. J. Pethick and H. Smith, in *Bose-Einstein Condensation in Dilute Gases* (Cambridge University Press, Cambridge, England, 2001); L. P. Pitaevskii and S. Stringari, *Bose-Einstein Condensation* (Oxford, New York, 2003); *Emergent Nonlinear Phenomena in Bose-Einstein Condensates Theory and Experiment*, edited by P. G. Kevrekidis, D. J. Frantzeskakis, and R. Carretero-González (Springer, New York, 2008).

[2] M. H. Anderson, J. R. Ensher, M. R. Matthews, C. E. Wieman, and E. A. Cornell, Science **269**, 198 (1995).

[3] C. C. Bradley, C. A. Sackett, J. J. Tollett, and R. G. Hulet, Phys. Rev. Lett. **75**, 1687 (1995).

[4] M. Edwards and K. Burnett, Phys. Rev. A **51**, 1382 (1995); F. Dalfovo and S. Stringari, *ibid.* **53**, 2477 (1996); P. A. Ruprecht, M. J. Holland, K. Burnett, and M. Edwards, *ibid.* **51**, 4704 (1995).

[5] V. I. Yukalov, E. P. Yukalova, and V. S. Bagnato, Phys. Rev. A **56**, 4845 (1997); **66**, 043602 (2002); M. Brtka, A. Gammal, and L. Tomio, Phys. Lett. A **359**, 339 (2006).

[6] Yu. S. Kivshar, T. J. Alexander, and S. K. Turitsyn, Phys. Lett. A **278**, 225 (2001).

[7] R. D'Agosta, B. A. Malomed, and C. Presilla, Laser Phys. **12**, 37 (2002).

[8] R. D'Agosta and C. Presilla, Phys. Rev. A **65**, 043609 (2002).

[9] V. V. Konotop and P. G. Kevrekidis, Phys. Rev. Lett. **91**,

230402 (2003).
[10] P. G. Kevrekidis, V. V. Konotop, A. Rodrigues, and D. J. Frantzeskakis, J. Phys. B **38**, 1173 (2005).
[11] G. Alfimov and D. Zezyulin, Nonlinearity **20**, 2075 (2007).
[12] D. E. Pelinovsky and P. G. Kevrekidis, e-print arXiv:cond-mat/0705.1016.
[13] L. D. Carr, J. N. Kutz, and W. P. Reinhardt, Phys. Rev. E **63**, 066604 (2001).
[14] J. J. García-Ripoll, G. Molina-Terriza, V. M. Pérez-García, and L. Torner, Phys. Rev. Lett. **87**, 140403 (2001).
[15] L.-C. Crasovan, G. Molina-Terriza, J. P. Torres, L. Torner, V. M. Pérez-García, and D. Mihalache, Phys. Rev. E **66**, 036612 (2002).
[16] L.-C. Crasovan, V. Vekslerchik, V. M. Pérez-García, J. P. Torres, D. Mihalache, and L. Torner, Phys. Rev. A **68**, 063609 (2003).
[17] L.-C. Crasovan, V. M. Perez-Garcia, I. Danaila, D. Mihalache, and Ll. Torner, Phys. Rev. A **70**, 033605 (2004).
[18] M. Mottonen, S. M. M. Virtanen, T. Isoshima, and M. M. Salomaa, Phys. Rev. A **71**, 033626 (2005).
[19] D. Mihalache, D. Mazilu, B. A. Malomed, and F. Lederer, Phys. Rev. A **73**, 043615 (2006).
[20] V. Pietila, M. Mottonen, T. Isoshima, J. A. M. Huhtamaki, and S. M. M. Virtanen, Phys. Rev. A **74**, 023603 (2006).
[21] G. Watanabe and C. J. Petick, Phys. Rev. A **76**, 021605(R) (2007).
[22] G. Herring, L. D. Carr, R. Carretero-González, P. G. Kevrekidis, and D. J. Frantzeskakis, Phys. Rev. A **77**, 023625 (2008).
[23] V. M. Pérez-García, H. Michinel, and H. Herrero, Phys. Rev. A **57**, 3837 (1998).
[24] G. Szegö, *Orthogonal Polynomials, American Mathematical Society, Colloquium Publication* (American Mathematical Society, Providence, RI, 1939), Vol. XXIII.
[25] *Handbook of Mathematical Functions*, edited by M. Abramovitz and I. A. Stegun (National Bureau of Standards, Washington, DC, 1972).
[26] I. M. Gelfand, *Lectures on Linear Algebra* (Dover, New York, 1989).
[27] T. Kato, *Perturbation Theory for Linear Operators* (Springer-Verlag, Berlin, 1966).
[28] R. S. MacKay, in *Hamiltonian Dynamical Systems*, edited by R. S. MacKay and J. Meiss (Adam Hilger, London, 1987), pp. 137–153.
[29] D. A. Zezyulin, G. L. Alfimov, V. V. Konotop, and V. M. Pérez-García, Phys. Rev. A **76**, 013621 (2007).
[30] C. M. Bender and S. A. Orszag, *Advanced Mathematical Methods for Scientists and Engeneers* (McGraw-Hill, New York, 1978).
[31] M. Kunze, T. Kupper, V. K. Mezentsev, E. G. Shapiro, and S. K. Turitsyn, Physica D **128**, 273 (1999).
[32] V. M. Eleonsky and V. G. Korolev, J. Phys. A **28**, 4973 (1995).
[33] V. M. Eleonsky and V. G. Korolev, Phys. Rev. A **55**, 2580 (1997).
[34] J. Morales, J. J. Peña, and A. Rubio-Ponce, Theor. Chem. Acc. **110**, 403 (2003).